Atom-Resolved Image of the $TiO_2(110)$ Surface by Noncontact Atomic Force Microscopy

Ken-ichi Fukui, Hiroshi Onishi, and Yasuhiro Iwasawa*

Department of Chemistry, Graduate School of Science, The University of Tokyo, Hongo, Bunkyo-ku, Tokyo 113, Japan

(Received 7 July 1997)

Atom-resolved images of a $TiO_2(110)$-(1×1) surface were obtained by noncontact atomic force microscopy (NC-AFM) in ultrahigh vacuum. In contrast to previous scanning tunneling microscopy studies, outermost atoms of bridge-bound oxygen ridges were observed as protruding rows by NC-AFM. A high-resolution image of the surface revealed that the bridging oxygen atoms ordered in (1×1) periodicity on terraces. Point defects of oxygen atoms were also imaged as dark spots. [S0031-9007(97)04584-5]

PACS numbers: 61.16.Ch, 68.35.Bs, 68.35.Dv

Metal oxides find applications in a variety of technologies where interfacial chemistry is critical to success, such as catalysis, gas sensors, photoelectrolysis, semiconductor or superconductor devices, etc. The oxide surfaces are, however, in general, heterogeneous and complicated. The inherent compositional and structural inhomogeneity of oxide surfaces makes the problem of identifying the essential issues for their functions extremely difficult. Scanning probe microscopy has particularly great potential to overcome the difficulty of heterogeneity, discriminating specific sites from the other sites in an atomic scale.

Following the invention of scanning tunneling microscopy (STM), several transition metal oxides have been subjects of real space imaging with atomic-scale resolution [1,2]. Rutile-type TiO_2 is a typical transition metal oxide and the (110) surface is one of the oxide surfaces most extensively studied including atom-resolved STM works by some groups [3–10]. A promising ability of STM in visualizing reactions on a metal oxide surface has been demonstrated even at elevated temperatures [11] and even in the presence of reactant gas ambients [12]. A practically important class of oxides (Al_2O_3, SiO_2, MgO, zeolites, etc.) is, however, out of range of the tunneling microscopy due to a nonconducting problem.

Atomic force microscopy (AFM) is, instead, applicable to the insulators. Experimentally, atomic-scale structures have been resolved by the AFM operated in contact mode. In this mode, the probing tip is in contact with the sample surface, and is scanned over the surface to keep the short-range repulsive force (normally 10 nN) between the tip and the surface to be constant. Under the assumption of a monoatomic tip, the relatively large loading of 10 nN theoretically results in the destruction of the tip apex [13]. It is, hence, assumed that the effective tip is composed of several atoms. Thus, the atomic-scale image obtained by the contact AFM is usually interpreted as the periodicity of the ordered surface.

On the other hand, noncontact (NC) atomic force microscopy provides an opportunity to observe atomic-scale singularities, such as adatoms and vacancies. This mode uses longer-range attractive force for regulation of tip-surface separation. Atomically resolved imaging of single atom vacancies has been demonstrated on semiconductor surfaces such as Si(111)-(7×7) [14–19], Si(100)-(2×1) [16], and InP(110) [19,20]. In the present Letter, we report NC-AFM topography of a metal oxide surface, $TiO_2(110)$-(1×1). Oxygen atoms protruding over the surface were individually visualized for the first time.

Since the magnitude of the attractive forces at relatively large distances may be considerably smaller than that of the short-range repulsion in the contact AFM, the method of interaction force detection in the NC-AFM is different from that of the contact AFM [21]. We used a frequency modulation technique introduced by Albrecht *et al.* [22]. As the cantilever vibrating with the resonant frequency in the vertical direction approaches the sample, the attractive force (with negative force gradient F') begins to work between the tip and the sample, resulting in the shift of the resonance frequency. A feedback signal is applied to the Z piezo to keep the frequency shift constant, which gives a topographic image of the surface.

The experiments were performed in an UHV-AFM (JEOL JAFM4500XT) equipped with an Ar^+ gun and low-energy election diffraction (LEED) optics. The base pressure was 1×10^{-8} Pa. Stiff silicon cantilevers with $f_0 = 260–290$ kHz and $k = 26–32$ N/m (NANOSENSORS) were used as the force sensor. These cantilevers had conductivity sufficient to observe STM by applying bias voltage between tip and sample and scanning the surface. A polished $TiO_2(110)$ wafer of $6.5 \times 1 \times 0.25$ mm^3 (Earth Chemicals Co.) was cleaned with cycles of Ar^+ sputtering (3 keV for 3 min) and UHV annealing at 900 K for 2 min. After the procedure, the surface exhibited a well contrasted (1×1) LEED pattern. The surface was observed with STM to confirm that wide terraces developed and (1×1) rows ran along the [001] direction.

Figure 1 shows a topographic image of the $TiO_2(110)$-(1×1) surface by NC-AFM. Bright rows parallel to the [001] direction were clearly observed at a regular interval of 0.65 nm. The corrugation of the rows along the $[1\bar{1}0]$

 0031-9007/97/79(21)/4202(4)$10.00

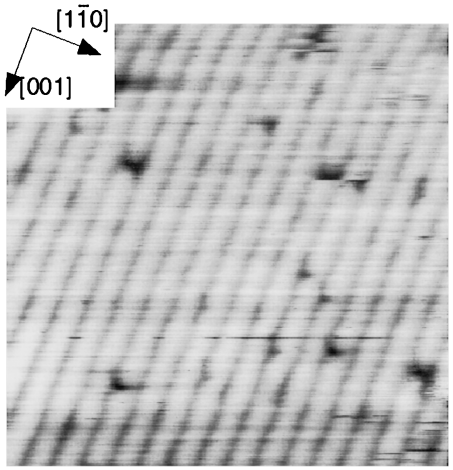

FIG. 1. Noncontact AFM image of the $TiO_2(110)$-(1×1) surface (10×10 nm^2). Oscillation amplitude of the cantilever was $\sim(30\ \text{nm})_{\text{p-p}}$ and the sample bias (V_s) was set for 0 V. The cantilever had a spring constant of 28 N/m and a resonant frequency of 270 kHz. The frequency shift (Δf) to obtain the topograph was $\sim$80 Hz.

direction was determined to be 0.07 ± 0.01 nm in cross section analysis. We interpret the bright rows as oxygen ridges protruding over the surface.

A stoichiometric structure, shown in Fig. 2, has been proposed for the (1×1) surface [23]. Recent surface x-ray diffraction [24], medium-energy backscattered electron diffraction [25], and an *ab initio* calculation of the energy minimized structure [26] studies support the model. The (1×1) surface contains two types of oxygen atoms, at bridge and in-plane positions, and two types of titanium atoms, fivefold and sixfold coordinated. Oxygen atoms bridging and covering the sixfold coordinated Ti atoms form ridges along the [001] axis. The fivefold coordinated Ti atoms are exposed to the surface. The (1×1) surface is, thus, composed of the alternative rows of the exposed Ti atoms and the bridging O ridges. The O ridges and Ti rows are aligned with a 0.65 nm separation, respectively. It has been established that the unoccupied states localized on the Ti rows were imaged as bright lines or spots in STM topography determined with positive sample bias voltages [9,27], though the Ti atoms are located 0.11 nm below the bridging oxygen atoms [24]. The reversal topographic contrast in STM, which is against the physical protrusion of the O ridges, is an artifact of "tunnel vision," resulting from the dominant contribution of electronic effects. In contrast, the NC-AFM image of Fig. 1 should reproduce physical topography of the surface, since the force regulating the tip-sample separation is largely element independent. It is, hence, a reasonable interpretation that the bridging oxygen atoms create the observed corrugation.

Figure 3 shows a high-resolution image of two terraces separated with a single height step, where axial corrugations were resolved along the bright lines. The periodicity along the row axis was 0.30 nm. The two-dimensional order of the bright spots, 0.65×0.30 nm^2, reproduces the alignment of the bridging oxygen atoms. Oxygen atoms on this surface were individually visualized for the first time by the use of NC-AFM, while STM is favorable for Ti atoms. This suggests the complementary roles of STM and NC-AFM in surface structure visualization.

Note that a slight plus bias of 0.5 V was applied to the sample to obtain the image in Fig. 3. However, the distance between the tip and the sample was controlled to keep the shift of resonance frequency of the cantilever (i.e., force gradient) constant. Güntherodt *et al.* [28,29] have reported that compensation of contact potential between

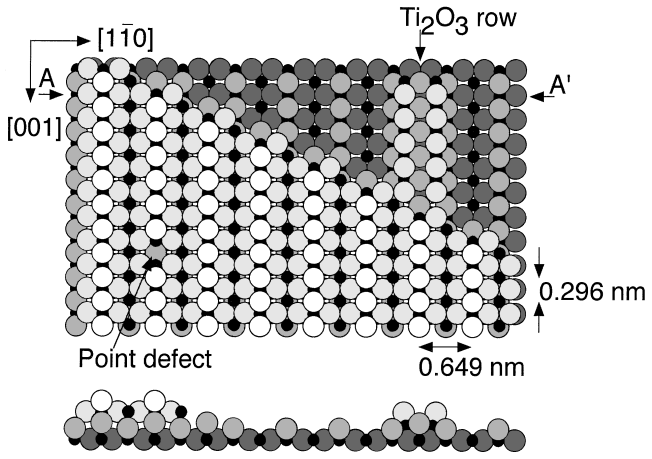

FIG. 2. A model of the $TiO_2(110)$-(1×1) surface with a single step, a point defect, and a Ti_2O_3 added row. Larger circles represent O atoms, with lighter shading representing higher atoms. Small solid circles represent Ti atoms. Bottom is a cross section of the surface at A-A'.

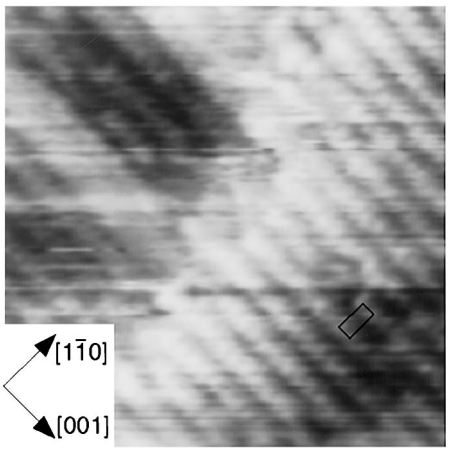

FIG. 3. Highly resolved noncontact AFM image of the $TiO_2(110)$-(1×1) surface (8.5×8.5 nm^2) with a single step. Oscillation amplitude of the cantilever was $\sim(30\ \text{nm})_{\text{p-p}}$ and the sample bias (V_s) was set for +0.5 V. The cantilever had a spring constant of 29 N/m and a resonant frequency of 280 kHz. The frequency shift (Δf) to obtain the topograph was $\sim$80 Hz.

tip and sample is essential to obtain a high contrast image of the atomic structure. The contact potential depends on material and contaminants such as an oxide layer. As cantilevers were used without cleaning in UHV, most of the surface of the Si tip must be covered with a native oxide layer. As far as we performed with different cantilevers, we could obtain the (1×1) rows at sample bias between -0.5 and $+2.5$ V.

In addition to the (1×1) rows of oxygen atoms, doubly wide rows were imaged by NC-AFM. Figure 4(a) shows a NC-AFM topography of two terraces separated with a single height step. Several double strands are observed on the lower terrace. Detailed analysis of the image of Fig. 4(a) provided further evidence for the interpretation of the contrast in NC-AFM. The wide row has been observed in STM studies on this surface [4–7,27], and which structure was interpreted as an extra row of Ti_2O_3 composition added on the stoichiometric (1×1) terrace as illustrated in Fig. 2 [27]. Recent results of electron stimulated desorption ion angular distribution measurement [30] and *ab initio* calculation [31] support the interpretation of the added rows. In the NC-AFM image of Fig. 4(a), the center of the Ti_2O_3 rows corresponds to the position of the bright lines of the upper terrace. The position of the (1×1) rows are guided with solid lines in Fig. 4(b). As illustrated in Fig. 2, the center of the Ti_2O_3 row stands in line with the bridging oxygen ridge on the upper terrace. This demonstrates that the bridging O atoms (ridges) of the (1×1) terrace are represented as the bright spots (lines) in the NC-AFM images.

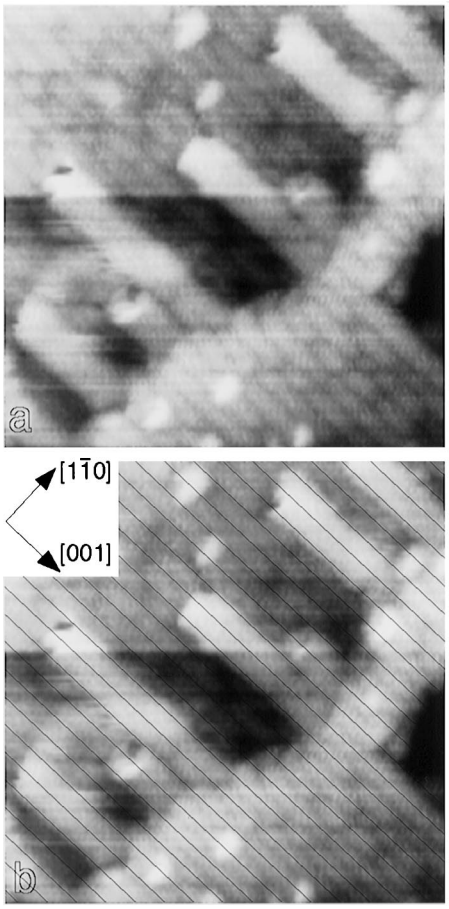

FIG. 4. (a) Noncontact AFM image of Ti_2O_3 added rows at a single step of TiO_2(110)-(1×1) surface $(14.5 \times 14.5\ nm^2)$. (b) Lines on the bright rows with 0.65 nm separation at the upper terrace were superimposed on the topograph in (a). Oscillation amplitude of the cantilever was $\sim(30\ nm)_{p\text{-}p}$ and the sample bias (V_s) was set for $+1.5$ V. The cantilever had a spring constant of 32 N/m and a resonant frequency of 290 kHz. The frequency shift (Δf) to obtain the topograph was $\sim$80 Hz.

Several dark sites were observed right on the bright lines in Figs. 1 and 3. They should be vacancies of the bridging oxygen atoms. Oxygen deficiency is easily induced on the TiO_2 surface by vacuum annealing at high temperatures [23]. It is thought that the removal of a bridging oxygen atom, which is less coordinated than the in-plane O atoms, is a favorable way to create a point vacancy of oxygen. The defect density on the (110) surface annealed at 1000 K was estimated at $8.7 \times 10^{13}\ cm^{-2}$ or $1.7 \times 10^{14}\ cm^{-2}$ in ultraviolet photoelectron spectroscopy [32] or ion scattering [33] studies. The coverage of dark sites counted in several NC-AFM images fell in the range of $(0.5\text{–}1.6) \times 10^{13}\ cm^{-2}$. Considering the lower annealing temperature of 900 K employed in the present study, the vacancy density determined with NC-AFM may be consistent with the reported values. Dark spots located out of the O-ridge center seen in Fig. 1 may be possibly the point vacancies of the in-plane O atoms.

In summary, we have succeeded in obtaining atom-resolved images of TiO_2(110)-(1×1) by noncontact AFM. In contrast to STM, bridging oxygen rows, which are outermost atoms on the surface, were observed as (1×1) protrusions by NC-AFM. Oxygen defects were imaged as dark sites in the (1×1) rows. These results demonstrate that NC-AFM can give more information of the surface structure combined with STM, and can be applied to nonconductive materials as a tool to explore chemical processes as well as surface structures in an atomic scale.

This work has been supported by CREST (Core Research for Evolutional Science and Technology) of Japan Science and Technology Corporation (JST).

*Corresponding author.
Electronic address: iwasawa@utsc.s.u-tokyo.ac.jp

[1] H. Onishi and Y. Iwasawa, in *Monograph on Chemistry for the 21st Century: Interfacial Science*, edited by M. W. Roberts (Blackwell Science, Oxford, 1997), p. 57.
[2] Y. Iwasawa, Stud. Surf. Sci. Catal. **101**, 21 (1996).
[3] G. S. Rohrer, V. E. Henrich, and D. A. Bonnell, Science **250**, 1239 (1990).

[4] M. Sander and T. Engel, Surf. Sci. **302**, L263 (1994).
[5] H. Onishi and Y. Iwasawa, Surf. Sci. **313**, L783 (1994).
[6] D. Novak, E. Garfunkel, and T. Gustafsson, Phys. Rev. B **50**, 5000 (1994).
[7] P. W. Murray, N. G. Condon, and G. Thornton, Phys. Rev. B **51**, 10 989 (1995).
[8] S. Fischer, A. W. Munz, K.-D. Schierbaum, and W. Göpel, Surf. Sci. **337**, 17 (1995).
[9] U. Diebold, J. F. Anderson, K.-O. Ng, and D. Vanderbilt, Phys. Rev. Lett. **77**, 1322 (1996).
[10] A. Berko and F. Solymosi, Langmuir **12**, 1257 (1996).
[11] H. Onishi, Y. Yamaguchi, K. Fukui, and Y. Iwasawa, J. Phys. Chem. **100**, 9582 (1996).
[12] H. Onishi and Y. Iwasawa, Phys. Rev. Lett. **76**, 791 (1996).
[13] F. F. Abraham and I. P. Batra, Surf. Sci. **209**, L125 (1989).
[14] F. J. Giessibl, Science **267**, 68 (1995).
[15] S. Kitamura and M. Iwatsuki, Jpn. J. Appl. Phys. **34**, L145 (1995).
[16] S. Kitamura and M. Iwatsuki, Jpn. J. Appl. Phys. **35**, L668 (1996).
[17] P. Güthner, J. Vac. Sci. Technol. B **14**, 2428 (1996).
[18] N. Nakagiri, M. Suzuki, K. Okiguchi, and H. Sugimura, Surf. Sci. **373**, L329 (1997).
[19] Y. Sugawara *et al.*, Appl. Surf. Sci. **113-114**, 364 (1997).
[20] Y. Sugawara, M. Ohta, H. Ueyama, and S. Morita, Science **270**, 1646 (1995).
[21] D. Sarid, *Scanning Force Microscopy with Application to Electric, Magnetic, and Atomic Forces* (Oxford University Press, New York, 1994).
[22] T. R. Albrecht, P. Grütter, D. Horne, and D. Rugar, J. Appl. Phys. **69**, 668 (1991).
[23] V. E. Henrich and P. A. Cox, *The Surface Science of Metal Oxides* (Cambridge University Press, Cambridge, England, 1994).
[24] G. Charlton *et al.*, Phys. Rev. Lett. **78**, 495 (1997).
[25] B. L. Maschhoff, J.-M. Pan, and T. E. Madey, Surf. Sci. **259**, 190 (1991).
[26] M. Ramamoorthy, D. Vanderbilt, and R. D. King-Smith, Phys. Rev. B **49**, 16 721 (1994).
[27] H. Onishi, K. Fukui, and Y. Iwasawa, Bull. Chem. Soc. Jpn. **68**, 2447 (1995).
[28] E. Meyer, L. Howald, R. Lüthi, H. Haefke, M. Rüetschi, T. Bonner, R. Overney, J. Frommer, R. Hofer, and H.-J. Güntherodt, J. Vac. Sci. Technol. B **12**, 2060 (1994).
[29] L. Howald, R. Lüthi, E. Meyer, and H.-J. Güntherodt, Phys. Rev. B **51**, 5484 (1995).
[30] Q. Guo, I. Cocks, and E. M. Williams, Phys. Rev. Lett. **77**, 3851 (1996).
[31] K.-O. Ng and D. Vanderbilt (private communication).
[32] R. L. Kurtz *et al.*, Surf. Sci. **218**, 178 (1989).
[33] J.-M. Pan, B. L. Maschhoff, U. Diebolt, and T. E. Madey, J. Vac. Sci. Technol. A **10**, 2470 (1992).